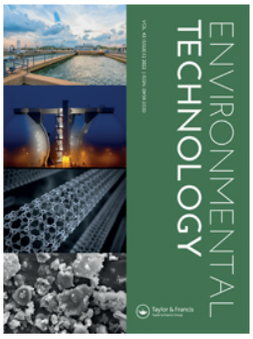

Environmental Technology

ISSN: (Print) (Online) Journal homepage: https://www.tandfonline.com/loi/tent20

Sticky stuff: biological cohesion for scour and erosion prevention

Rob Schindler, Richard Whitehouse & John Harris

To cite this article: Rob Schindler, Richard Whitehouse & John Harris (2022): Sticky stuff: biological cohesion for scour and erosion prevention, Environmental Technology, DOI: 10.1080/09593330.2022.2052362

To link to this article: https://doi.org/10.1080/09593330.2022.2052362

© 2022 The Author(s). Published by Informa UK Limited, trading as Taylor & Francis Group

View supplementary material

Published online: 11 Apr 2022.

Submit your article to this journal

Article views: 160

View related articles

View Crossmark data

Full Terms & Conditions of access and use can be found at
https://www.tandfonline.com/action/journalInformation?journalCode=tent20

ENVIRONMENTAL TECHNOLOGY
https://doi.org/10.1080/09593330.2022.2052362

OPEN ACCESS Check for updates

Sticky stuff: biological cohesion for scour and erosion prevention

Rob Schindler [a], Richard Whitehouse[b] and John Harris[b]

[a]School of Geography, Earth & Environmental Science, University of Plymouth, Plymouth, UK; [b]Coasts & Oceans, HR Wallingford, Howbery Park, Wallingford, UK

ABSTRACT

This study examines the potential for biological cohesion to arrest scour erosion at marine infrastructure. Biological cohesion occurs naturally in sedimentary environments, and is caused by extracellular polymeric substances (EPS) which result from the life cycles of microorganisms. EPS is known to dramatically increase the resistance of natural biomediated sediment to erosive hydrodynamic forces. In this study, we test, for the first time, whether EPS can be deliberately added to a sediment to mitigate against scour erosion – a process we term 'biostabilisation'. A systematic laboratory experiment is used to investigate the effects of an EPS additive on scour erosion around a monopile in a sand substrate. Results show that increasing EPS content causes a progressive reduction in equilibrium scour depth, the volume of excavated material and the timescale required to reach equilibrium scour morphology. These parameters are linearly related to EPS content, showing that the effects of EPS on the physical processes required for erosion to occur are concentration dependent. It can be concluded that biostabilisation offers a potential new ecologically engineered, nature-based solution to a range of scour and erosion scenarios. The economic and environmental advantages are discussed, and a methodology for biostabilisation use in individual erosion mitigation scenarios is proposed.

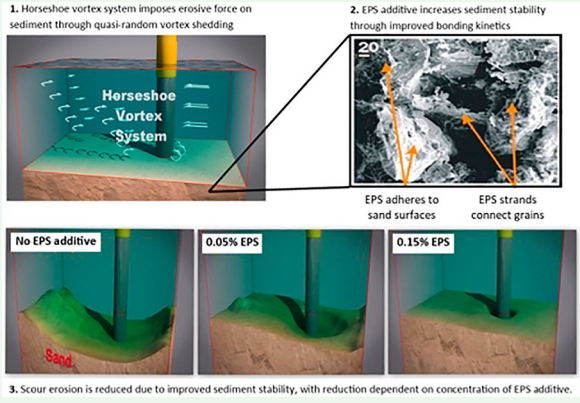

ARTICLE HISTORY
Received 24 December 2021
Accepted 20 February 2022

KEYWORDS
Biostabilisation; Erosion; Scour protection; EPS; Monopile; Cohesion

1. Introduction

Engineered structures in fluvial, coastal and offshore locations have very different physical characteristics than the natural habitats they replace. Globally, an estimated 1.0–3.4 million km^2 of seascape has been modified by the installation of engineered coastal structures [1]. The predicted expansion of coastal hardening by 50–76% over a 25-year period [2] will further damage coastal marine ecosystems already experiencing multiple pressures [3] from our use of the marine environment for socio-economic gain, including from oil and gas production, offshore wind energy, tidal and wave energy, communication networks, power cables, pipelines and the commensurate increase in supporting coastal infrastructure.

A key aspect of the design of infrastructure in subaqueous environments is protecting it from physical damage resulting from the hydrodynamic forcing of waves, currents and tides. Scour erosion is a ubiquitous threat to offshore wind farms, oil and gas rigs, bridge piers, coastal defenses, seafloor infrastructure such as pipelines and cables (amongst others). It occurs because structures disrupt the flow field, resulting in a

CONTACT Rob Schindler robert.schindler@plymouth.ac.uk
Supplemental data for this article can be accessed online at https://doi.org/10.1080/09593330.2022.2052362.

© 2022 The Author(s). Published by Informa UK Limited, trading as Taylor & Francis Group
This is an Open Access article distributed under the terms of the Creative Commons Attribution-NonCommercial-NoDerivatives License (http://creativecommons.org/licenses/by-nc-nd/4.0/), which permits non-commercial re-use, distribution, and reproduction in any medium, provided the original work is properly cited, and is not altered, transformed, or built upon in any way.

higher capacity for erosion of the substrates in which the structure is sited. Hydrodynamic conditions leading to scour include flow separation and the generation of coherent turbulent structures, focusing of wave energy or currents by structural alignments, downward-directed breaking waves, wave pressure differentials and intensified orbital velocities of reflected waves [4]. In addition, the installation of infrastructure can weaken natural sediment structure, reducing the critical force required for erosion.

Scour can be reduced by modifying the structure to reduce the strength of turbulent vortices that result in increased erosive force. Even with these improvements, some degree of scour is inevitable, and reinforcement of the substrate in which the structure is placed is required. Typically, methods of protecting against scour erosion rely on 'hard engineering' approaches to armor sediments, including the positioning of concrete, large rocks, gabion baskets, plastic matting and rock mattresses on the affected site. Consequently, the environmental 'footprint' of a structure includes the materials used to protect it. 'Hard engineering' methods of scour mitigation have shortcomings for: (1) Economic reasons: cost of material and transport to site, cost of specialist vessels; (2) Practical reasons: distance to offshore sites, uncertainty of sea operations, need for precise sub-sea assembly; (3) Environmental reasons: disruption of geomorphological processes, damage to ecological communities, reliance of carbon-intensive methods [5,6].

The improved capacity to predict the extent of scour in a range of hydrodynamic conditions and sediment types has allowed scour mitigation methods to be optimized to reduce economic costs and environmental impacts. Notably, predictions that assume a cohesionless substrate (e.g. [7,8]) have been replaced by those that better parameterize the effects of variations in sedimentological properties. For instance, fine cohesive fractions, common within all sedimentary environments [9], impart physical cohesion that may reduce the rate and equilibrium depth of scour as it takes a large number of shear stress cycles to overcome the hydrostatic and electromagnetic bonds between clay particles e.g. [10,11].

More recently, it has been recognized that *biological* cohesion mediates sediment erosion, transport, deposition and consolidation in aquatic sedimentary ecosystems [12]. Biological cohesion is imparted by a matrix of extracellular polymeric substances (EPS) which result from the life cycles of microorganisms capable of colonizing various soft (i.e. sediment or soil) surfaces that exist across diverse environments, including streams and rivers, lakes, estuaries and marine environments [13].

Substrates containing EPS exhibit considerably greater resistance to erosion compared with both cohesionless and physically cohesive (clay, silt) sediments. Field studies, laboratory experiments and theoretical analysis have allowed greater precision in quantifying the effects of biological cohesion on sediment stability. Surficial EPS biofilms (1–5% dry mass) completely suppress sediment transport until critical shear stress is sufficiently high to cause catastrophic failures in the biofilm [14]. Sub-surface concentrations of EPS of <1% by mass may increase sand stability by two orders of magnitude compared with physical cohesion imparted by clay/silt fractions [15–17]. Even trace amounts of EPS (<0.1% by mass) can increase resistance to erosion ten-fold in sandy estuaries and limit the development of fundamental morphological disturbances such as current ripples [18] and dunes [17] at concentrations of <0.5%.

The discrepancy between the stability induced by physical (clay) and biological (EPS) cohesion results from the superior bonding kinetics offered by EPS. Where clay platelets form loose linear assemblages under electrostatic bonding, biopolymer molecules adhere to sediment grain surfaces, form elastic 'bridges' linking grains, fill void space and ultimately envelope grains [17]. EPS bonding kinetics are particularly pronounced in sediment finer than about 2 mm (clay, silt, sand) [12]. Consequently, biomediated sediment matrices display viscoelastic properties. They undergo both reversible elastic responses and irreversible deformation, depending strongly on the forces acting on the EPS matrix. Although the magnitude of the elasticity modulus and the viscosity vary among mixed-species biofilms [19], the qualitative viscoelastic responses to shear stress are consistent [20]. Increased cohesion under shear stress (known as strain hardening) has been observed in biofilms [21].

Isolating individual constituents of naturally biomediated sediments is challenging as they contain an immense range of components that each require different extraction methods [22] which may damage cells [23]. EPS were initially denoted 'extracellular polysaccharides' but were renamed, as it became clear proteins, nucleic acids, lipids and other biopolymers such as humic substances are also present [24].

If follows that replication of the EPS bonding kinetics found in natural systems is a potential tool for reducing erosion in substrates that are prone to unwanted erosion. In this paper we pose the question: Can we deliberately add EPS to cohesionless fine-grained sediments as a means to mitigate against erosion?

In practical terms the propagation of benthic microphytobethos to produce the required EPS additive is

unnecessary. An increasing range of EPS and behaviorally similar substances (cellulose derivatives, plant extracts), all of which we group under the term 'biopolymers', are produced commercially for industry. Applications include: adhesives or binders, bulking agents and coagulants for food; pharmaceutical and cosmetic industries, and; finishing, binding and lubricants in the textile, paper, construction, and drilling industries.

While natural EPS can contain considerable amounts of proteins that, together, can far exceed the polysaccharide content on a mass basis, it seems to be mainly the polysaccharide fraction that provides mechanical stability [25]. Notably, polysaccharides from an extensive range of bacterial species from diverse environments have been isolated and characterized [26], with many used for industrial and commercial purposes. Most are long molecules, linear or branched, with a molecular mass of 0.5×10^6 daltons to 2×10^6 daltons [23].

We present unique experiments that systematically examine how the deliberate addition of a polysaccharide EPS to cohesionless sediment to impart biological cohesion – henceforth termed 'Biostabilisation' – may be used to reduce scour around a structure, as a first step to realizing the potential of this new method of scour reduction for a wide-range of engineering purposes in aquatic substrates. We show that such an approach may reduce or negate the need for hard engineering measures and the associated economic, practical and environmental shortcomings.

2. Methods & materials

2.1. Selection of monopiles for the case study

Monopiles offer an ideal case study for the initial deployment of bioengineered sediments because: (1) their idealized structure allows data comparison across numerous other experiments, regardless of scale; (2) findings can be validated by comparing scour data from real-world observations (e.g. [4]). Further, (3) monopiles are ubiquitously used in fluvial, coastal and offshore structures (e.g. bridge piers, oil and gas rigs, offshore windfarms). Notably, scour erosion is a primary concern in the delivery of offshore wind farms due to the high capital cost of foundation installation and innovation in foundations has been identified as a key research priority because it offers the second greatest potential for reducing costs after turbine manufacture [27].

Scour erosion at monopiles in a current is driven by an adverse pressure gradient, generating three-dimensional flow separation of the upstream boundary layer [28]. A 'horseshoe' vortex system develops in the junction region between the bed and the monopile and oscillates randomly around the monopile, inducing highly elevated means and fluctuations in bed shear stress. This increases the erosional force acting on the substrate surface, resulting in local scour processes, with periodic vortex shedding in the wake of the cylinder capable of lifting and transporting eroded material [29].

2.2. Flume, monopile & flow conditions

Experiments were performed in Plymouth University's COAST Laboratory's recirculating sediment flume (l $20.0 \times w$ 0.6 m) which includes a recessed scour pit (l $2.1 \times w$ $0.36 \times d_{sed}$ 0.26 m; Figure 1; see [11]). The model monopile was 0.048 m in diameter, D. Assuming a prototype monopile diameter of 2.0 m yields a geometric ratio of 41.67. When applied to a 10 m prototype water depth this yields a model depth, d, of 0.24 m. The monopile was segmented to allow detailed scans of the final scour morphology to be obtained without obstruction of the protruding monopile. Bespoke sediment trays were fitted with a model monopile and then filled with different biostabilised substrates before insertion into the sediment pit. Fresh water was used in the tests.

Trial scour experiments in pure sand were used to select the current velocity that maximized the rate of scour erosion associated with the monopile (i.e. an adverse pressure gradient sufficiently strong to induce horseshoe vortices to develop) but where the freestream velocity was insufficient to cause erosion (i.e. 'clear water' conditions, see [7]). Subsequently, a Nortek Vectrino 2 + acoustic Doppler velocity profiler was used to characterize the velocity profile at the centerline above the flat flume bed at the position of the monopile. The depth-mean downstream velocity, U, was 0.20 m s^{-1}, shear velocity, $U^* = 0.014$ m s^{-1}, bed shear stress, $\tau_b =$ 0.198 N m^{-2}, Froude number, $Fr = 0.13$, depth-mean Reynolds number, $Re = 26{,}880$ and depth-mean pile Reynolds number, $Re_D = 9680$. Input velocity was constant and bed slope was zero throughout each experiment.

2.3. Biostabilised sediments

Biostabilised substrates were prepared using powdered *Xanthan gum*, a polysaccharide EPS derived from the bacteria *Xanthomonas campestris*, and used elsewhere as a proxy for naturally occurring EPS in the laboratory [15,17,18]. Xanthan gum is produced by fermentation based on renewable carbohydrate raw materials, such as glucose syrup, sucrose, or starch. After glucose exhaustion, the culture medium is heat sterilized to kill the *Xanthomonas* cells and inactivate enzymes produced

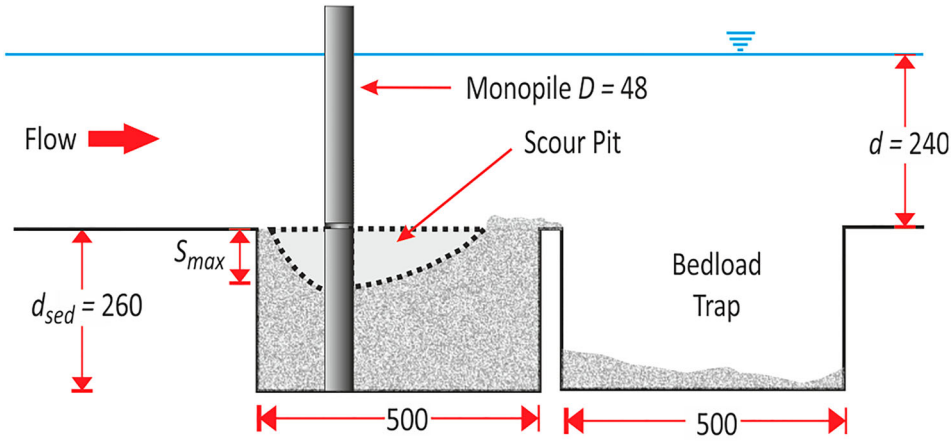

Figure 1. Side view schematic of experimental setup. All units in mm.

by the bacterium which would otherwise degrade the polysaccharides and damage xanthan's rheological properties [30]. Consequently, xanthan is considered biologically inert [31]. It has a large molecular weight (2,000,000 daltons), which is at the upper end of those found in naturally occurring polysaccharides [23]. Xanthan gum shows pseudoplasticity of solution, minimal change of viscosity over a wide range of temperatures, solubility and stability in both acid and alkaline solutions, and viscosity stability over a wide pH range [32] making it a durable product suitable for use in coastal waters.

Eight sand-EPS mixtures were examined spanning EPS contents of 0.0125% < $\boldsymbol{b_0}$ < 0.5000% (see Table 1). This range of concentrations is below that typical of surficial biofilms (1% < $\boldsymbol{b_0}$ < 5%) [14], but aligns well with sub-surface concentrations ($\boldsymbol{b_0}$ < 1%) responsible for dramatic increases in sediment stability in natural sediments [15–18]. Each fraction was mixed dry with unimodal medium sand (median percentile, D_{50} = 230 µm) using a motorized drum mixer (Creteangle Multi-Flow Mixer) for 20 min (sufficient to reach homogeneity) before 12.5 L of water were added to saturate the mixture. The baseline 'Sand Only' run was used as a control.

Initial surface shear strength was measured using a 20 mm diameter shear vane in the uppermost 25 mm of sediment at ten locations towards the margins of each substrate prior to each experiment and averaged to yield a representative mean shear strength value, τ.

2.4. Scour measurements

Scour development was measured using a laser point gauge mounted on a manual traverse. The sampling rate was 10 Hz and each measurement took 1.0 s. The laser outputs data as voltage which required conversion to millimeters using a linear calibration equation. Measurements were made along the 530 mm centerline at 10 mm increments. Previous experiments assessing scour around monopiles in currents have shown that achieving a stabilized, equilibrium scour is extremely

Table 1. Mean shear strength, $\boldsymbol{\tau}$, bedload *EPS Loss* and scour variables for each experiment: Normalized equilibrium maximum scour depth, S_{eqm} / D and timescale of scour, T_s, for each run using best-fit relationship derived from Equation (1a).

b_0 (%)	τ (kPa)	*EPS Loss (%)*	S_{eqm}/D	T_s (mins)	R^2	E_{eqm}/D (mm)	T_e (mins)	R^2	T_s / T_e
0 (Sand)	1.11 (0.24)	–	1.632 (0.166)	6.41 (4.96)	0.70	248.4 (68.68)	95.71 (66.35)	0.87	14.93
0.0125	1.41 (0.33)	0.91	1.567 (0.175)	9.456 (7.36)	0.78	198.5 (33.9)	100.05 (41.26)	0.97	10.58
0.025	1.65 (0.43)	0.94	1.503 (0.093)	10.14 (4.33)	0.94	200.4 (54.4)	156.8 (80.60)	0.97	15.46
0.05	1.23 (0.21)	0.82	1.357 (0.107)	60.31 (15.06)	0.98	91.8 (22.4)	79.27 (22.39)	0.98	1.31
0.075	1.39 (0.23)	0.87	1.280 (0.582)	221.40 (162.40)	0.97	74.9 (18.2)	174.2 (76.01)	0.98	0.79
0.1	0.94 (0.32)	0.78	1.212 (0.494)	299.40 (173.56)	0.99	29.0 (19.3)	186.7 (217.44)	0.88	0.62
0.125	1.22 (0.35)	0.71	1.229 (0.640)	530.8 (725.20)	0.98	16.4 (3.56)	90.94 (50.31)	0.93	0.17
0.15	0.99 (0.33)	0.79	0.633 (0.283)	292.90 (188.5)	0.99	12.9 (1.3)	100.2 (29.86)	0.95	0.34
0.5	1.21 (0.42)	No Data	0.066 (0.013)*	5.15 (8.34)*	0.07*	3.80 (0.3)†	30.69 (12.00)†	0.57†	–

Notes: Normalized equilibrium excavation area, E_{eqm} / D and timescale of excavation, T_e, for each run using best-fit relationship derived from Equation (1b). Confidence intervals shown in parentheses. Underline indicates Equation (1) is unsuitable for description of relationship.
*Data is better suited to a power-law relationship, see Section 3.2.
†Data is better suited to a 2nd-order polynomial, see Section 3.3.

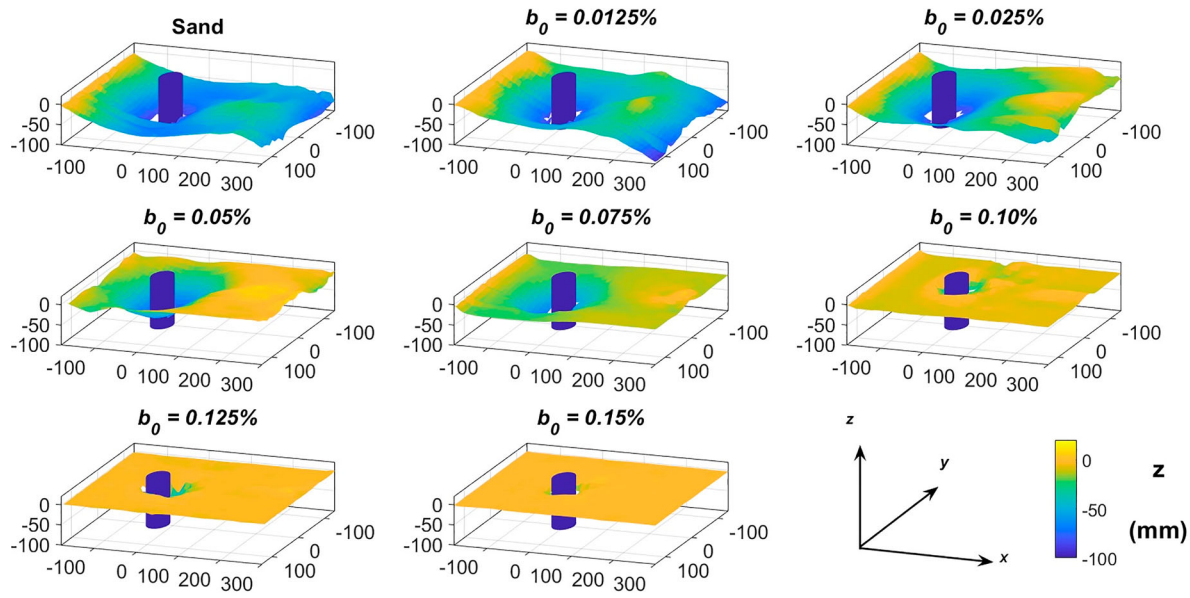

Figure 2. Surface plots of final scour surfaces ($t = 300$ min) for each experimental run. $b_0 = 0.5\%$ is omitted.

time consuming and consequently limits the number of experimental runs that can be undertaken [33]. This was also the case here, particularly for high EPS content substrates. Resulting data indicated that 5 h was sufficient to reach equilibrium scour depth for $0\% < b_0 < 0.05\%$ by mass. For higher EPS concentrations, data were extrapolated to obtain predictions of equilibrium scour parameters.

Once the current was applied, measurements were made at pre-set intervals over 5 h ($t = 300$ min) that were biased towards initial scour development. The laser head was removed from the water between transects to minimize flow disruption (transects took approximately 120 s to complete; sampling height of laser head $z = 100$ mm or $z/d \sim 0.4$). Note that the closest centerline measurements are 6 mm (half the width of the laser head) upstream/downstream of the monopile. Each transect included a known datum and an initial baseline measurement was taken before the current was initiated. After each experiment the current was terminated, the monopile top segment removed, and a detailed scan of the whole substrate surface was made over a 530×280 mm area (10×10 mm grid).

2.5. Characterization of eroded material

A bedload trap was used to capture eroded substrate material. Because the sediment pit does not span the width of the flume some material was transported at the flume margins. For this reason, the total mass and volume of material excavated and transported as bedload could not be obtained. However, the relative contributions of sand and EPS to captured material after each experimental run were established through measurements of the carbohydrate content (a proxy for EPS), using a standard Dubois assay [34].

3. Results

3.1. Final 3D morphology

Figures 2 and 3 show 3D surface plots and the centerline morphology of the final sediment surfaces ($t = 300$ min), respectively. (Note that the evolving centreline morphology of each experiment can be found in Supplementary Figure 1.) For each surface, maximum scour depth, S_{max}, is located at the monopile. The Sand Only run exhibits the greatest degree of scour around the monopile in terms of its depth and lateral extent. The scour zone is conical in shape with smooth sides. Scour is also evident at the downstream lip of the sediment tray, indicating that the turbulence field is capable of erosion well beyond the downstream extent of the substrate. This resulted in local erosion at the downstream lip of the sediment tray not directly associated with the monopile. Scour depth and gradient are greatest on the stoss side, but the lee side scour zone extends further with a shallower but constant gradient, typical of scour around monopiles (e.g. [28]). Lee-side erosion is concentrated at the margins of the sediment surface, aligned with vortex streets generated around the side of the monopile.

EPS contents of $b_0 = 0.0125\%$ & $b_0 = 0.025\%$ show a progressive reduction in the depth and lateral extent of scour, although both show erosion at the downstream

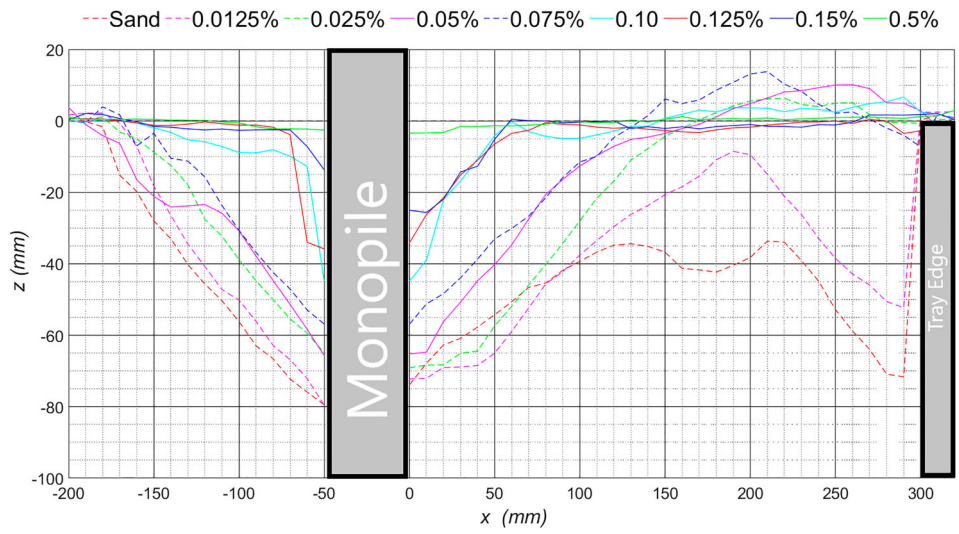

Figure 3. Centreline morphology of final scour surfaces ($t = 300$ min) for each experimental run. All units in mm.

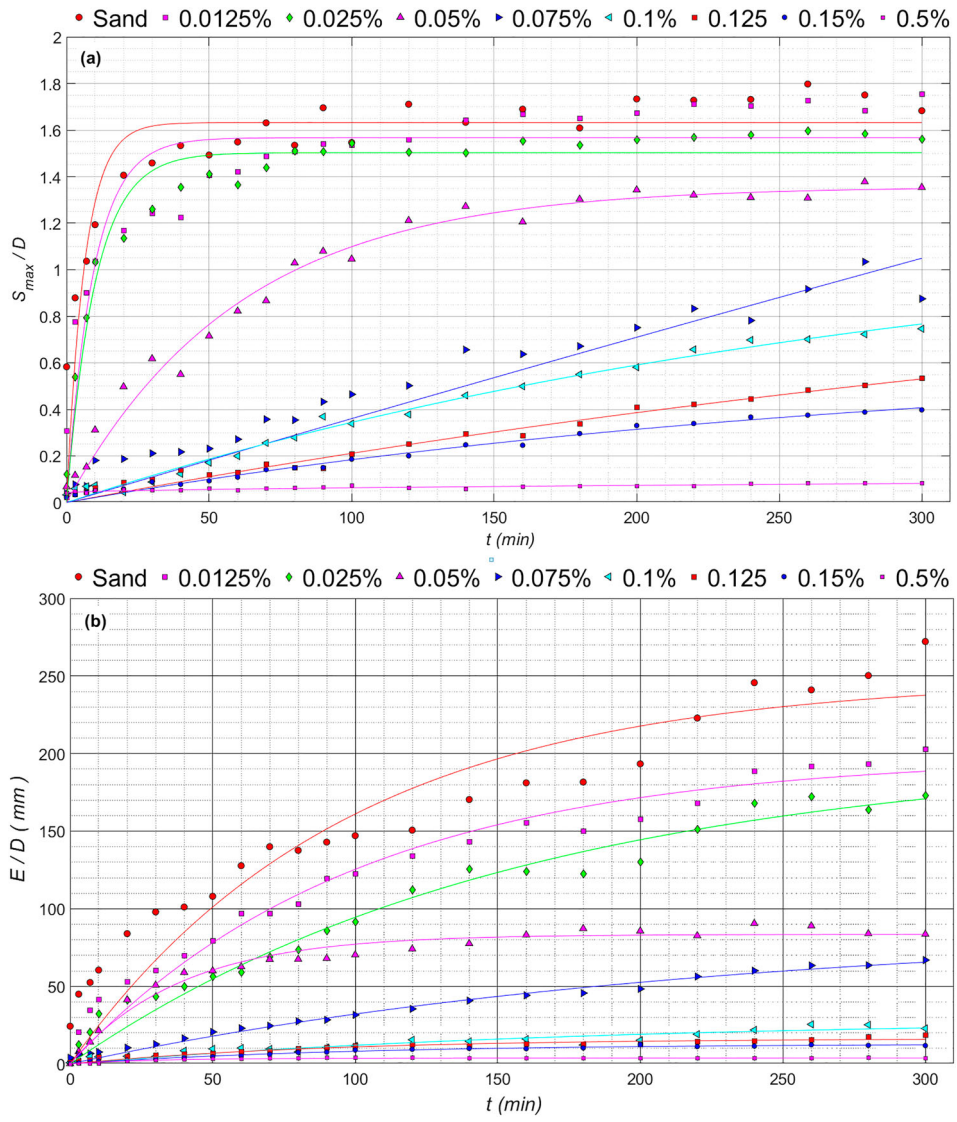

Figure 4. Change in (a) normalized maximum scour depth, S_{max} / D, and (b) normalized excavation area, E_{max} / D across the 5 h (t = 300 min) experiments, including best-fit curves derived from Equation (1).

lip of the sediment tray. Stoss-side slopes exhibit shallower gradients than the Sand Only case, resulting from lower scour depths at the upstream face of the monopile. Conversely, the gradients of the lee-side slopes are steeper because the downstream extent of scour is lower. Both scour surfaces exhibit lee-side lateral erosion associated with vortex streets. For $b_0 =$ 0.0125% centerline erosion occurs from the monopile to the downstream end of the sediment surface. However, the minimum lee-side elevation is $z =$ −8.5 mm and located closer to the monopile ($x =$ 185 mm) compared with the Sand Only case which erodes to a minimum of $z = -33.6$ mm at $x = 206$ mm. For $b_0 = 0.0125\%$ centerline erosion extends to $x =$ 170 mm, after which eroded material is deposited in the lee-side above the baseline to a maximum height of $z = +6.4$ mm and $x = 210$ mm.

Where $0.05 \leq b_0 \leq 0.15\%$ erosion is limited to the monopile with no erosion at the downstream lip of the sediment tray. The relative size and depth of the scour hole continues to diminish as EPS content increases. The slopes of the hole become steeper, as seen in substrate containing physically cohesive sediment [10]. The volume and elevation of sediment deposited above the baseline in the lee decreases as EPS content increases. Erosion is very limited for $b_0 = 0.5\%$. The maximum scour depth of $z = -3.4$ mm occurs on the lee face of the monopile and erosion is restricted to $-100 \leq x \leq +80$ mm.

3.2. Scour depth

Maximum scour depth, S_{max}, along each centerline transect was determined for each point in time, t, for each experiment. In each instance S_{max} was located at the monopile, typically on the stoss side. Time development curves of normalized maximum scour depth, S_{max}/D, are shown in Figure 4a.

Both the rate of growth of S_{max} /D and its value at each time step diminish with EPS content. Where $0 \leq b_0 \leq 0.05\%$, the development of scour occurs rapidly initially due to the strong feedback effect of flow turbulence [35]. Values become asymptotic with time through an exponential decaying time dependence [36], indicating that values after 5 h are approaching or have reached equilibrium. This indicates that EPS cohesion modifies the physical processes causing erosion to limit final scour depth compared to cohesionless materials.

Values for $b_0 \geq 0.075\%$ do not asymptote over the 5 h data set. In order to establish whether these data also conform to the same exponential decaying time dependence, and to derive equilibrium values for all experiments, a curve of the following form

$$S_{max}/D(t) = S_{eqm}/D(1 - e^{-t/T_s}) \tag{1a}$$

was applied to the time-development curves of S_{max}/D to yield normalized equilibrium scour depth, S_{eqm}/D, and timescale of scour, T_s [37]. The fits minimize mean absolute difference between measurements. The results are shown in Table 1 with corresponding curves shown in Figure 4a.

Broadly, S_{eqm}/D exhibits a negative relationship to b_0. For the Sand Only case, $S_{eqm}/D = 1.632$ which corresponds to assumptions for cohesionless materials of $S_{eqm}/D \sim 1.75$ (e.g. [8]), although it shows the weakest fit to Equation (1a) ($R^2 = 0.70$). This is principally due to deviation from the fit over $10 \leq t \leq 60$ mins where measured values are below predicted values. Where $b_0 = 0.0125\%$ ($R^2 = 0.78$) the fit also over-predicts for the same period. However, for $0.025 \leq b_0 \leq 0.15\%$ fits are excellent ($R^2 > 0.90$). S_{eqm}/D decreases with each increase in b_0 with the exception of $b_0 =$ 0.10% ($S_{eqm}/D = 1.121$) to $b_0 = 0.125\%$ ($S_{eqm}/D = 1.229$). However, where $b_0 = 0.50\%$ Equation (1a) performs poorly ($R^2 =$ 0.07), and the curve is best described by a power function ($S_{max}/D = 0.0001525\ t^{0.574} + 0.042$, $R^2 = 0.92$, shown on Figure 4a).

With the exception of $b_0 = 0.15\%$ the time-scale of scour, T_s, is positively related to b_0. Notably, despite similar scour depths, T_s increases by 77% between b_0 $= 0.10\%$ ($T_s = 299.40$ min) to $b_0 = 0.125\%$ ($T_s =$ 530.80 min). Conversely, T_s drops by 81% between $b_0 = 0.125\%$ ($T_s = 530.80$ min) and $b_0 = 0.15\%$ ($T_s =$ 292.90 min) despite a very good fit ($R^2 = 0.99$).

3.3. Excavation area

While S_{max} is a key parameter in any scour evaluation it is important to recognize that it is a single value representative of one point in space. It is also informative to consider the amount of material excavated during scour development which also takes account of changes in morphology of the scour pit.

The excavation area, E – defined as the area of material lost below the baseline ($z = 0$ mm) – was determined for each point in time for each run. Time-development curves of normalized excavation area, E / D, are shown in Figure 4b. Note that for experiments where $0.0125 \leq b_0 \leq 0.075\%$ erosion associated with the downstream lip of the sediment tray was omitted and elevations along the centerline were assumed to be zero. The same form of curve determined from Equation (1a) was used to establish equilibrium excavation area,

E_{eqm}, and timescale of excavation, T_e, modified as

$$E/D(t) = E_{eqm}/D(1 - e^{-t/T_e}) \quad (1b)$$

The results are shown in Table 1. Best-fit curves are superimposed in Figure 4b. The E_{eqm}/D curves show a similar developmental form to S_{eqm}/D curves. Equation (1b) shows the poorest fit for Sand Only ($R^2 = 0.87$), where E/D is underestimated for $0 \le t \le 70$ mins and overestimated for $70 \le t \le 220$ mins. For $b_0 = 0.1\%$ ($R^2 = 0.88$), measured values are above predicted values where $0 \le t \le 100$ mins. Where $b_0 = 0.50\%$ Equation (1b) performs poorly ($R^2 = 0.59$), and the curve is best described by a 2nd-order polynomial ($E/D = -0.0001019b_0^2 + 0.03814b_0 + 0.7471$, $R^2 = 0.79$), shown on Figure 4(b). All remaining experiments show fits to Equation (1b) of $R^2 \ge 0.92$.

3.4. EPS concentration, shear strength and EPS Loss

Initial EPS content and mean shear strength are poorly correlated (Figure 5, $R^2 = 0.05$), with no discernable relationship between variables established through a curve-fitting exercise. Mean shear stress values for biostabilised substrates vary around the Sand Only value, with most values falling within its 95% confidence band (1.11 kPa ± 0.12 kPa). Largest mean shear strength of 1.65 kPa was measured for $b_0 = 0.025\%$, and minimum shear strength of 0.94 kPa was measured for $b_0 = 0.1$.

Figure 6 shows the relationships between each equilibrium scour parameter and b_0 (no values for $b_0 = 0.5\%$). A curve-fitting exercise showed that S_{eqm}/D is negatively linearly related to b_0 (Figure 6a, $R^2 = 0.83$). Using the regression equation, the addition of 0.1% EPS results in a decrease in S_{eqm}/D of 0.42, or S_{eqm} of 20.16 mm. T_s is linearly related to b_0 (Figure 6b, $R^2 = 0.83$) with the principal deviation resulting from high and low T_s values for $b_0 = 0.125\%$ and $b_0 = 0.15\%$, respectively. The addition of 0.1% EPS results in an increase in T_s of 307 min.

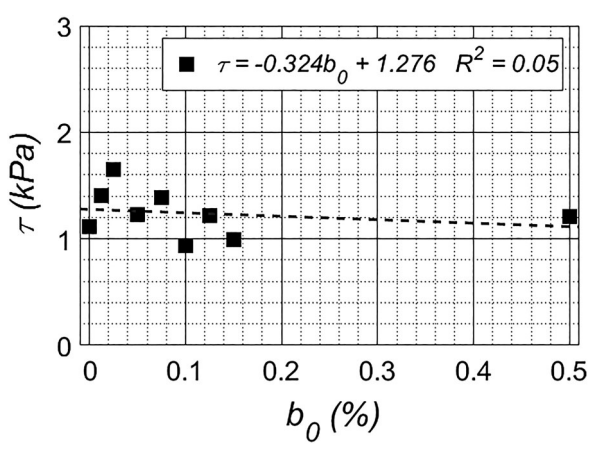

Figure 5. Relationship between initial EPS concentration, b_0, and mean shear strength, τ.

Broadly, E_{eqm}/D exhibits a negative linear relationship to b_0 (Figure 6c, $R^2 = 0.90$), as seen for S_{eqm}/D. The addition of 0.1% EPS results in a decrease in E_{eqm}/D of 162 mm, or E_{eqm} of 7776 mm^2. However, time-scale of excavation, T_e, does not exhibit a relationship with b_0 (Figure 6d, correlation $R^2 = 0.00$). Values range from 186.7 min for $b_0 = 0.075$ to 86.7 min for $b_0 = 0.1\%$. For $0 \le b_0 \le 0.0.025\%$, T_s/T_e values (Table 1) are >10, i.e. T_e is an order of magnitude larger than T_s values. For $b_0 = 0.05\%$ $T_s/T_e = 1.31$. Where $b_0 \ge 0.075\%$, time-scales of scour are greater than time-scales of excavation.

Table 1 and Figure 7 show the relative *EPS Loss* from captured eroded material (where 0% is no EPS removed and 100% is all EPS removed; not applicable to the Sand Only run). All experiments exhibit a marked reduction in EPS content of the eroded substrate compared with initial values. *EPS Loss* is above 71% in all cases. It exhibits a moderate, negative linear relationships with b_0 ($R^2 = 0.69$).

4. Discussion

4.1. Effects of EPS content

The experiments conclusively prove that biological cohesion imparted by EPS modifies scour dynamics in an otherwise cohesionless sediment matrix. Increasing EPS content causes a clear, progressive reduction in scour depth, the area subject to scour and hence volume of excavated material over a 5 h time period. Furthermore, EPS does not merely limit the rate of scour, ultimately yielding the same equilibrium form [33]. Instead, equilibrium scour depth and excavation area are linearly related to initial EPS content, showing that EPS cohesion modifies the physical processes causing erosion to limit final scour morphology compared to cohesionless substrates.

The strong linear relationships between EPS content, equilibrium scour depth and timescales of scour indicates that the effects of EPS are concentration-dependent for $b_0 \le 0.15\%$. That is, EPS bond strength and the number of bonds acting to retain sand particles in the substrate matrix is proportional to the availability of EPS material. The depth, extent and timescale of scour development decrease with EPS content because there is less void space between sand particles and a greater number of EPS bonds that physically link them.

The consistent loss of EPS from eroded material indicates that erosion is dependent on the removal of

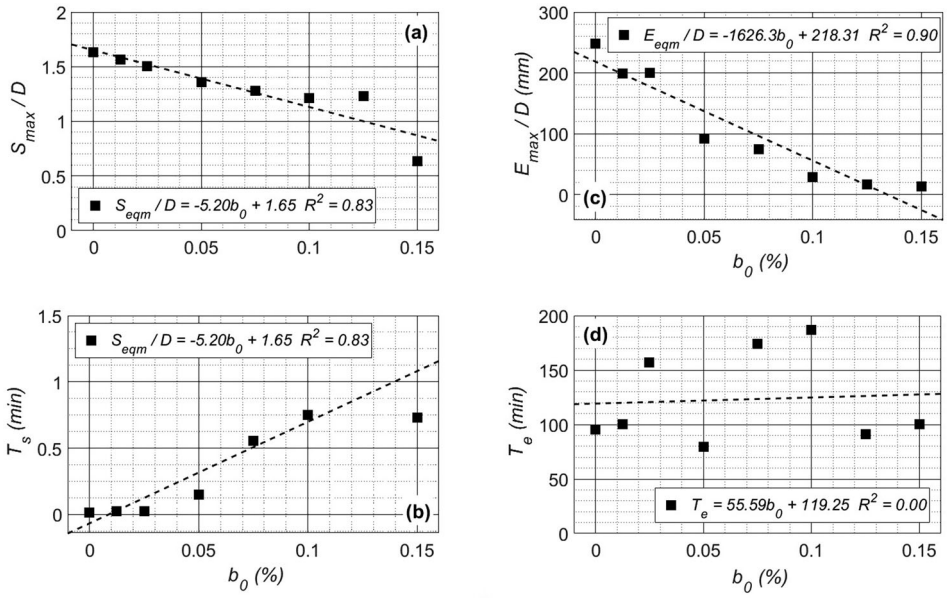

Figure 6. Relationship between initial EPS concentration, b_0, and equilibrium excavation parameters derived from Equation (1): (a) Normalized maximum equilibrium scour depth, S_{max} / D, (b) time-scale of scour, T_s, (c) Normalized equilibrium excavation area, E_{max} / D (d) Time-scale of excavation, T_e.

individual sand grains from the sand-EPS matrix, rather than the removal of larger sand-EPS aggregates. Initially, the uppermost layer of sediment is exposed to the flow. Erosion is triggered when the shear stress is sufficiently strong to break EPS bonds, exposing the next layer of sediment for EPS removal. This agrees with previous experimental work on ripples and dunes in EPS-sand mixtures which indicate that the removal rate of EPS from bedform troughs limits bedform growth [17,18]. The process is analogous to the selective entrainment or 'winnowing' of mud from cohesionless grains that controls erosion rate and depth in physically cohesive substrates [9,11].

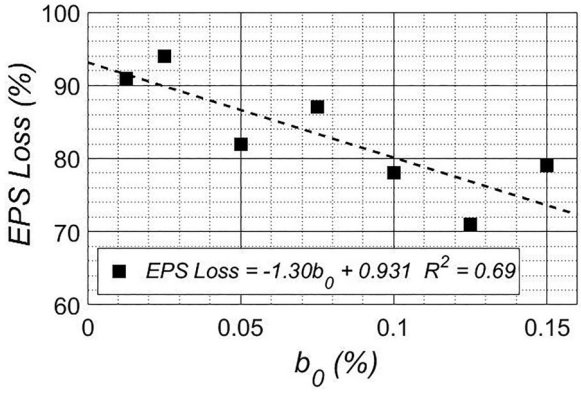

Figure 7. Relationship between bedload *EPS Loss* and initial EPS concentration, b_0. Not applicable to Sand Only condition.

The depth and spatial extent of the scoured area are controlled in this manner. Turbulence structure around a monopile in a current causes a large spatial gradient in mean and instantaneous stresses acting on the sediment surface [28]. Maximum scour depth occurs at the monopile where the horseshoe vortex system is focused. The stresses decline with distance from the monopile until, ultimately, they are not sufficient to break EPS bonds. Consequently, under clear water conditions, the liberation of sand particles available for entrainment will diminish in rate with distance from the monopile until the pressure gradient is no longer sufficient to generate stresses that cause EPS loss, and hence erosion.

Because the current, depth and slope are the same between experiments the distribution of stresses remains constant (albeit with the evolving scour morphologies modifying the local flow domain). The disparity in equilibrium scour morphology between EPS contents is because the strength of the sand-EPS matrices depends on the relative proportions of each component.

It follows that higher concentrations of EPS generate more and/or stronger bonds between sand grains. It is not simply the case that a critical stress needs to be overcome to immediately induce the removal of a sand grain for entrainment; the strong, linear relationship between b_0 and T_s indicates that duration of the stress needed to cause entrainment becomes longer as EPS concentration increases.

At concentrations $0.075 \leq b_0 \leq 0.15\%$, considered the upper range for EPS in sub-surface estuarine environments, EPS can envelope individual sand grains [12,17]. The EPS concentrations in this study fall either side of this value suggesting that sand grains are increasingly embedded in EPS sockets as b_0 increases. This may explain why for $b_0 = 0.50\%$ scour was both extremely limited and that its development did not conform to Equation (1). An increased proportion of sand grain surface coated in EPS may also explain why an increasing quantity of EPS is retained on sand grains after entrainment.

Scour development is asymptotic, and conforms to scour development in both cohesionless and partially cohesive sediments noted elsewhere (e.g. [35,36]). Physical cohesion using kaolin clay in place of EPS was investigated in parallel experiments using the same experimental setup and flow conditions [11]. Comparison of data across each study reveals that similar S_{eqm}/D values are found where kaolin content, $f_0 = 2.5\%$ and $0.05 < b_0 < 0.075\%$, while comparable E_{eqm}/D values occur at $f_0 = 2.5\%$, $0.025 < b_0 < 0.05\%$, and $f_0 = 12.5\%$, $b_0 = 0.075\%$. Further, E_{eqm}/D at $f_0 = 15\%$ is four times greater than $b_0 = 0.15\%$. In addition, time-scales required to reach similar equilibrium scour depths are an order of magnitude greater for biostabilised sediments than those containing clay. We can conclude that by mass EPS is around two orders of magnitude more effective at preventing erosion than kaolin clay.

It is reasonable to assert that these differences are the result of stronger bonding kinetics that take longer to break prior to sand grain entrainment. Examinations of clay (kaolin) and EPS (Xanthan gum) bonds in mixed sand-clay-EPS matrices based on high-resolution Cryo-SEM imagery provide a useful comparison [17]. Clay particles exhibit edge-to-plate bonds and stack between sand grains, filling voids. EPS has a much larger bonding potential because it actually adheres to sand grain surfaces, and sand grains become physical linked by web-like strands or encased in EPS 'sockets'.

Notably, sediments with physically cohesive components can change in character depending on the relative proportions of cohesionless and cohesive fractions. Medium sand – kaolin matrices are grain supported (i.e. sand grains are in contact) at low kaolin concentrations but become matrix-supported (i.e. sand grains are separated by kaolin platelets) at higher values, citing a threshold of ~15% by mass [9]. A parallel change in EPS-sand matrix behavior may also occur when EPS concentrations are sufficiently high to encase individual grains, although the transition may not be as abrupt.

Physical cohesion can incur irregular scour morphology (e.g. [35]). In comparison, the scour holes in this study remain conical in shape, with smooth sides, a symmetrical shape either side of the centerline and a bias towards erosion in the lee of the monopile. Observations of sand-kaolin scour [11], which are directly comparable to those presented here, showed that the degree of irregularity in scour morphology increased with kaolin content. Comparison of both studies shows that the strength of fit of Equation (1b) was stronger for sand-EPS mixtures than for sand-kaolin mixtures. Further, they show that scour development was well correlated with mean surface shear strength across clay contents of $0 < f_0 < 15\%$ by mass, as noted elsewhere (e.g. [38]). Based on this study, improved resistance to erosion in biostabilised sediment is not governed by an increase in shear strength. Instead, we may speculate that stability is induced by the linking of sand grains that allow forces acting on the sediment surface to be distributed throughout adjacent grains. Visual observation and physical manipulation of the biostabilised sediments indicate they are viscous, and exhibit a degree of elasticity.

4.2. Economic & logistical advantages of bioengineered sediments

From an economic standpoint the deployment of biostabilised sediments may reduce manufacturing costs of existing scour mitigation methods, and reduce installation time and related logistical expenses associated with the complexity of offshore operations. Specifically, biostabilised sediments offer the following advantages: (1) EPS can be added to existing site sediments to minimize installation time and costs; (2) Potentially, very little EPS is required to stabilize a sediment – avoiding issues of bulk and mass; (3) EPSs have little mass and are stable so can be easily transported and stored; (4) Biostabilisation may reduce physical changes to the affected site, reducing impacts on natural habitats in the construction phase and long-term. Further, (5) many EPS types and behaviorally similar additives exist and are (6) produced at very low cost so there is scope to tailor the choice and concentration of additive to the specific context. (7) Waste (e.g. dredged) sediments may also be re-purposed to create biostabilised substrates to create a circular economy in marine operations.

If biostabilised sediments are found to have few negative environmental and ecological impacts (see 4.4) they may also be less subject to permitting and licensing restrictions compared with existing methods, and allow deployment of infrastructure in environmentally protected waters.

4.3. Developing methods of biostabilization

This study is limited to (1) a single biopolymer under (2) a single current (3) at a single type of structure in (4) freshwater and was (5) undertaken under scaled conditions. Nevertheless, the study provides a framework for biostabilisation as a method for a broad range of erosion control applications.

The structures of biopolymer substances are complex, from single to mixed molecules with diverse functional groups, linked in linear or branched chains, where secondary structures are defined by chemical and physical interactions [39]. Thus, bonding kinetics are expected to differ between biopolymer types. Common industrial biopolymer types are (1) polysaccharide EPS (e.g. xanthan, pullulan, dextrans, curdlan), (2) exopolysaccharide EPS (e.g. gellan, urdla), (3) cellulose derivatives (e.g. methylcellulose, carboxymethylcellulose), and (4) plant extracts (e.g. starches, guar gum, agar). Furthermore, molecular structures are commonly modified for different functionality, with variants offering different viscosity, salt-tolerance, pseudoplasticity, dispersion, and capacity to bind with particles. Given the findings herein, future work will examine the efficacy of other biopolymers in stabilizing sediments.

The influence of physical cohesion imparted by cohesive sediments is well established. Consequently, a variety of methods have been used to parameterize cohesive or mixed-cohesive sediments their mechanical, geotechnical or erosion properties [4]. Conversely, geotechnical/rheological parameterization of biopolymer-sediment mixtures is poor. When in solution, EPS rheology is concentration-dependent and influences viscosity, elasticity and cohesiveness [39]. However, the micro-scale interactions between particles and EPS are poorly understood and does not extend to materials principally comprised of particles [40].

Therefore, parameterizations of different particle-rich biopolymer mixtures are needed to generate a full understanding of biophysical processes governing the erosion of biostabilized sediments. Findings herein show that surface shear strength is an inappropriate measure of the stability induced by EPS bonding kinetics. An immediate practical approach may be to quantify biostabilised sediment stability through a universal, dimensionless parameter describing the relative change in yield strength, which subsumes the effects of a range of geotechnical/rheological parameters. Such an approach would facilitate quantitative comparison of different biopolymer-sediment mixtures for practical applications. Understanding the yield strength of different biopolymer-sediment mixtures in the absence of a structure would provide a baseline data set for practical application. It follows that the concentration of different additives required to prevent erosion could be determined for individual erosion scenarios with known hydraulic forcing.

Understanding the broad differences in mineral grain arrangement and contact, pore space and particle-biopolymer bonding kinetics across different grain characteristics would help elucidate the mechanics underlying enhanced stability. This could be achieved through their microscopic examination with surface scanning electron microscopy (e.g. [17]) or x-ray tomography which could provide a qualitative analyses of three-dimensional matrix structure. This information can be used to qualitatively elucidate different critical erosion thresholds, erosion rates and biopolymer losses.

Further characterization should include the effects of salinity on the behavior of biopolymers, which are only partially known [41]. We can expect behavioral differences between seawater and freshwater conditions for some materials as the type and concentration of cations can modify the interaction between biopolymers and particles [42].

The size of the vortex network responsible for erosion depends on velocity and diameter of the structure because higher Reynolds numbers cause larger boundary layers and earlier separation [29]. Waves may also intensify scouring. Their effect is highly dependent on wave height, period and orbital velocity at the sediment bed which dictate the size and lifespan of the horseshoe vortex, and hence the force and extent of shear stresses that result in erosion [28].

While determination of the yield strength of biostabilised sediments in unobstructed flows is independent of scale, the dynamic length scales of turbulent structures responsible for erosion around structures do not exhibit dynamic similitude at different scales. For instance, the relative equilibrium scour depth diminishes as monopile diameter increases [43]. Consequently, the precise effects of scale on erosion for individual applications need to be determined through a transition from small-scale experiments such as those presented herein to larger-scale testing and, ultimately, full-scale field trials.

Thus, future research should employ (1) different biopolymer types at (2) different concentrations, and (3) examine erosion and scour dynamics under different hydrodynamic conditions (currents, waves and combined conditions) in (4) freshwater and saline environments and (5) at different scales. Unifying the effects of biopolymers as a single parameter would provide a practical means of quantifying changes in stability induced by different treatments. It follows that, for

different hydrodynamic conditions and substrates, the degree of scour can be predicted based on the concentration of biopolymer and optimized to prevent scour for individual scenarios.

Moreover, this study does not consider the durability of the biostabilised sedimentary matrix beyond the length of each experimental run. In naturally biomediated sediments the EPS may be (1) winnowed from the sediment and become dissolved within the flow [18], (2) adhere to suspended load as a component of aggregated sand grains [44], (3) remain bound to bedload [45] or (4) be consumed by flora and fauna [13]. This should be established for a wide range of environments. Mechanisms of delivery also need addressing, including the potential to adapt existing technologies.

4.4. Environmental & ecological considerations

The addition of a polysaccharide EPS only partially replicates the complex matrix comprising biological cohesion in natural sedimentary systems. However, results confirm that xanthan gum significantly strengthens the sediment matrix through use of the bonding kinetics resulting from a polysaccharide fraction. As such, Biostabilisation can be considered an ecologically engineered, nature-based solution to erosion in fine sedimentary environments. It can be compared favourably to the environmental impacts of existing 'hard' scour mitigation strategies that also contributes to 'net-zero' carbon emission goals, and addresses the need to reconcile socioeconomic and environmental priorities.

Shifts from natural, soft sediment to hard, artificial (e.g. concrete, plastic, larger sediments, steel) substrates: (1) causes the direct loss of benthic habitats; (2) interrupts geomorphological and ecosystem functionality; (3) reduces capacity of ecosystems to store and degrade nutrients [6], and; (4) encourages the spread of invasive non-native species (e.g. [46]). Hard substrates also carry a 'trophic footprint'. Notably, (5) hard substrates propagate invertebrates, which can negate the primary production of 130 m^2 of seafloor for every 1 m^2 [1]. Coastal hardening also (6) promotes sessile biomass which, on average, results in the loss of the energy equivalent of 26 m^2 of ocean surface primary production for every 1 m^2 of hard infrastructure per day [47]. These effects continue long-after the useable lifespan of the structure.

Biostabilisation can directly reduce carbon emissions that result from the production of concrete, metals and plastics. Larger substrates, e.g. rocks, are also used to armour erodible sediments. Combined, these measures rely on the transport of large volumes of materials from their source to site. As outlined in Section 4.2, the effectiveness of biopolymer bonding kinetics means that they are required in very small quantities. Combined with their deployment in existing site sediments, or waste sediments sourced from dredging, biostabilisation compares well in terms of carbon output through both manufacturing and distribution, and can contribute to 'net zero' carbon emission goals.

However, the potential of biopolymer additives to modify benthic ecology must be established. They may alter the structure of microbial communities and the functioning (primary productivity, energy transfer, biotic interactions) of surface and subsurface sediments.

Such effects may not be negative. They may promote the succession of other flora and fauna, resulting in increased sediment stability and ecosystem regeneration, particularly in sediments disturbed through engineering. The formation and maintenance of structured multicellular microbial communities crucially depends on the presence of EPS [26]. EPS promotes the existence of longterm mixed-species microconsortia, providing biodiversity on a small scale. Polysaccharides and proteins both contribute. They are adhesive, which promotes colonization of biotic and abiotic surfaces by planktonic cells. Further, they protect cyanobacterial nitrogenase from the harmful effects of oxygen and against some grazing protozoa [23]. The resulting aggregation of bacterial cells enables bridging between cells, the temporary immobilization of bacterial populations, the development of high cell densities and cell–cell recognition. They also promote sorption of organic compounds, facilitating the accumulation of nutrients from the environment and the sorption of xenobiotics (thus contributing to environmental detoxification). It has been theorized that cell lysis and subsequent local decomposition of the EPS matrix might be advantageous for the biofilm population, creating new pores and channels that improve nutrient access [48]. In addition, many EPS are hygroscopic and seem to retain water entropically rather than through specific water-binding mechanisms, which has been proven to maintain photosythetic activity of bacterium under wet-dry cycles [49].

Owing to their complexity, EPS are only slowly biodegradable, and complete degradation of all components requires a wide range of enzymes. Extracellular enzymatic activity within biofilm matrices can render dissolved polymers and particulate substrates bioavailable for further decomposition. These include α-glucosidase, β-glucosidase, *N*-acetyl-β-dglucosaminidase and Chitobiosidase. However, these effects have yet to be properly quantified [50].

Polysaccharides store excess carbon under unbalanced carbon to nitrogen ratios and accumulate, retain and stabilize enzymes. Conversely, proteins promote enzymatic activity and degradation of structural EPS [23]. In that respect, use of a purely polysaccharide additive limits the environmental degradation of the structural bonds that yield improved stability.

Xanthan gum is a highly stable polysaccharide that is not easily degraded by most micro-organisms [51]. The stability of xanthan gum may be affected when soil organisms at high concentrations are in contact with it for one month, or when certain strains of bacteria isolated from sewage sludge and soil release enzymes that could degrade it [51]. Consequently, xanthan gum may be degradable, but not readily biodegradable. Further, due to its large molecular weight (2,000,000 daltons), it is not expected to be bioavailable. Therefore, xanthan gum is not expected to bioaccumulate and does not pose an appreciable environmental hazard and is considered non-toxic to aquatic organisms [52].

Thus, if the added biopolymer shares similar characteristics to xanthan gum, it is likely to be resistant to degradation and consumption by benthic organisms.

Future work will examine a range of other biopolymers to establish the most appropriate type, concentration and extent of different biostabilised substates required for individual applications. Armed with this knowledge, the implications of biostabilisation on marine and freshwater ecology at different spatial and temporal scales may be considered.

5. Conclusion

Biostabilisation simulates the biological cohesion found in nature, offering an ecologically engineered, nature-based solution to that of erosion in fine sedimentary environments. The experiments presented herein are the first attempt to employ biological cohesion to mitigate against scour and erosion. We use a classical study of erosion around a monopile to demonstrate that very small amounts of a polysaccharide EPS equating to natural benthic communities (e.g. [16]) are sufficient to reduce the rate, depth and extent of scour.

We may conclude that the potential for biostabilisation to be employed as a measure to reduce erosion is considerable, and that at it may have the capacity to reduce or prevent scour completely in a range of scour/erosion scenarios in fluvial, coastal or offshore locations. The strong, linear relationships between EPS content and scour parameters offer a simple means of developing methods of matching EPS concentrations to meet known hydrodynamic forcing for individual erosion mitigation scenarios.

Biostabilised sediments used as backfill with EPS, in a surface layer akin to natural 'biofilms', or in combination with other hard engineering measures may be extremely effective, economically attractive and ecologically more sensitive compared with traditional scour mitigation strategies and requires additional research.

Acknowledgements

The authors are grateful to the following members of staff at the University of Plymouth: Victor Kuri for laboratory analyses of eroded material and discussion of EPS; Daniel Conley and Sean Comber for valuable reviews of the draft manuscript; Stuart Stripling for enabling the experimental work, and; the COAST Laboratory technical staff. Contributions of Richard Whitehouse and John Harris were funded through HR Wallingford's scour research programme, which also provided the laser used for bed profiling.

Disclosure statement

No potential conflict of interest was reported by the authors.

Funding

This study was supported by the Marine Institute, Plymouth University through Round 6 of the Higher Education Innovation Fund, provided by Research England.

Data availability

Due to the nature of this research, participants of this study did not agree for their data to be shared publicly, so supporting data is not available.

ORCID

Rob Schindler http://orcid.org/0000-0001-6870-0845

References

[1] Bugnot AB, Mayer-Pinto M, Airoldi L, et al. Current and projected global extent of marine built structures. Nat Sustain. 2020;4:33–41.
[2] Floerl O, Atalah J, Bugnot AB, et al. A global model to forecast coastal hardening and mitigate associated socioecological risks. Nat Sustain. 2021;4:1060–1067.
[3] Mayer-Pinto M, Cole VJ, Johnston EL, et al. Functional and structural responses to marine urbanization. Environ Res Lett. 2018;13:014009.
[4] Harris JM, Whitehouse RJS. Marine scour: lessons from nature's laboratory. In: L Cheng, S Draper, H An, editor. Proceedings of the seventh international conference on scour and erosion. London: Taylor & Francis; 2015. p. 12–21.
[5] Firth L, Knights AM, Bridger D, et al. Ocean sprawl: challenges and opportunities for biodiversity management

in a changing world. Oceanogr Mar Biol. 2016;54:189–262.
[6] Heery EC, Bishop MJ, Critchley LP, et al. Identifying the consequences of ocean sprawl for sedimentary habitats. J Exp Mar Biol Ecol. 2017;492:31–48. doi:10.1016/j.jembe.2017.01.020.
[7] Richardson EV, Davis SR. Evaluating scour at bridges, Rep. No. FHWAIP—90-017 (HEC 18), Federal Highway Administration, Washington, 1995.
[8] den Boon JH, Sutherland J, Whitehouse RJS, et al. Scour behaviour and scour protection for monopile foundations of offshore wind turbines. London: EWEC; 2004.
[9] Baas JH, Davies AG, Malarkey J. Bedform development in mixed sand and mud: The contrasting role of cohesive forces in flow and bed. Geomorphology. 2013;182:19–32.
[10] Harris JM, Whitehouse RJS. Scour development and large-diameter monopiles in cohesive soils: evidence from the field. J Waterw Port Coast Ocean Eng. 2017;143:123–142.
[11] Schindler RJ, Stripling S, Whitehouse RJS, et al The influence of physical cohesion on scour around a monopile. In: J Harris, RJS Whitehouse, S Moxon, editors. Scour and Erosion. London: , CRC Press; 2016. p. 325–334.
[12] Paterson DM, Hope JA, Kenworthy J, et al. Form, function and physics: the ecology of biogenic stabilization. J Soils Sediments. 2018;18:3044–3054. doi:10.1007/s11368-018-2005-4.
[13] Gerbersdorf SU, Koca K, de Beer D, et al. Exploring flow-biofilm-sediment interactions: assessment of current status and future challenges. Water Res. 2020;185:116182, doi:10.1016/j.watres.2020.116182.
[14] Hagadorn JW, McDowell C. Microbial influence on erosion, grain transport and bedform genesis in sandy substrates under unidirectional flow. Sedimentology. 2012;59:795–808. doi:10.1111/j.1365-3091.2011.01278.x.
[15] Tolhurst TJ, Gust G, Paterson DM. The influence of an extracellular polymeric substance (EPS) on cohesive sediment stability. In: JC Winterwerp, C Kranenburg, editors. Proceedings in marine science series vol. 5. Amsterdam: Elsevier; 2002. p. 409–425.
[16] Gerbersdorf SU, Westrich B, Paterson DM. Microbial extracellular polymeric substances (EPS) in fresh water sediments. Microbial Ecol. 2009;58:334–349.
[17] Parsons DR, Schindler RJ, Hope JA, et al. The unrecognized role of bio-physical cohesion on subaqueous bedform size. Geophysl Res Lett. 2016;43:1566–1573.
[18] Malarkey J, Baas JH, Hope JA, et al. The pervasive role of biological cohesion in bedform development. Nat Commun. 2015;6:6257.
[19] Klausen MM, Thomsen TR, Nielsen TL, et al. Variations in microcolony strength of probe-defined bacteria in activated sludge flocs. FEMS Microbiol Ecol. 2004;50:123–132.
[20] Stoodley P, Cargo R, Rupp CJ, et al. Biofilm material properties as related to shear-induced deformation and detachment phenomena. J Ind Microbiol Biotechnol. 2003;29:361–367.
[21] Hohne DN, Younger GJ, Solomon MJ. Flexible multifluidic device for mechanical property characterization of soft viscoelastic solids such as bacterial biofilms. Langmuir. 2009;25:7743–7751.
[22] Flemming HC, Neu TR, Wozniak D. The EPS matrix: the house of biofilm cells. J Bacteriol. 2007;189:7945–7947.
[23] Flemming H-C, Wingender J. The biofilm matrix. Nat Rev. 2010;8:623–633.
[24] Allison DG, Sutherland IW, Neu TR. EPS: what's in an acronym? In: A McBain, D Allison, M Brading, AH Rickard, J Verran, J Walker, editor. Biofilm communities: order from chaos? Cardiff: BioLine; 1998. p. 381–387.
[25] Frølund B, Palmgren R, Keiding K, et al. Extraction of extracellular polymers from activated sludge using a cation exchange resin. Water Res. 1996;30:1749–1758.
[26] Sutherland IW. The biofilm matrix – an immobilized but dynamic microbial environment. Trends Microbiol. 2001;9:222–227.
[27] Renewables Advisory Board, Value breakdown for the offshore wind sector; 2010.
[28] Sumer BM, Fredsøe J. The mechanics of scour in the marine environment. Singapore: World Scientific; 2002.
[29] Baker CJ. The oscillation of horseshoe vortex systems. J Fluids Eng. 1991;113:489–495.
[30] Hublik G. Xanthan. In: K Matyjaszewski, M Moller, editor, Polymer science: a comprehensive reference. 2012;10: 221–229.
[31] Dintzis FR, Babcock GE, Tobin R. Studies on dilute solutions and dispersions of the polysaccharide from Xanthomonas campestris NRRL B-1459. Carbohydrate Res. 1970;13:257–267.
[32] Rocks K. Xanthan Gum. Food Technol. 1971;25:22–31.
[33] Briaud JL, Ting CK, Chen C, et al. SRICOS: prediction of scour rate in cohesive soils at bridge piers. J Geotech Env Eng. 1999;125:237–246.
[34] Dubois M, Giles KA, Hamilton JK, et al. Colorimetric method for determination of sugars and related substances. Analy Chem. 1956;28:380–356.
[35] Debnath K, Chaudhuri S. Laboratory experiments on local scour around cylinder for clay and clay-sand mixed beds. Eng Geol. 2010;111:51–61.
[36] Soulsby RL. Dynamics of marine sands. London: Thomas Telford; 1997.
[37] Whitehouse RJS, Sutherland J, O'Brien D. Seabed scour assessment for offshore windfarms. Proceedings Third International Conference on Scour and Erosion (November 1 - 3, 2006), Amsterdam, The Netherlands.. 2006: 698–707.
[38] Kamphuis JW, Hall KR. Cohesive material erosion by unidirectional current. J Hydr Eng. 1983;109:49–61.
[39] Bourne MC. Food texture and viscosity. London: Academic Press; 2002.
[40] Genovese GB, Lozano JE, Rao MA. The rheology of colloidal and noncolloidal food dispersions. J Food Science. 2007;72:R11–R20.
[41] Dario AF, Hortencio LMA, Sierakowski MR, et al. The effect of calcium salts on the viscosity and adsorption behavior of xanthan. Carbohydr Polym. 2011;84:669–676.
[42] Higiro J, Herald TJ, Alavi S, et al. Rheological study of xanthan and locust bean gum interaction in dilute solution: effect of salt. Food Res Int. 2007;40:435–447.
[43] Ettema R, Kirkil G, Muste M. Similitude of large-scale turbulence in experiments on local scour at cylinders. J Hyd Eng. 2006;132:33–40.
[44] Manning AJ, Langston WJ, Jonas PJC. A review of sediment dynamics in the severn estuary: influence of flocculation. Mar Pollut Bull. 2010;61:37–51.

[45] Paterson DM. Short-term changes in the erodibility of intertidal cohesive sediments related to the migratory behaviour of epipelic diatoms. Limnol Oceanogr. 1989;34:223–234.
[46] Glasby T, Connell S, Holloway M, et al. Nonindigenous biota on artificial structures: could habitat creation facilitate biological invasions? Mar Biol. 2007;151:887–895.
[47] Malerba ME, White CR, Marshall DJ. The outsized trophic footprint of marine urbanization. Front Ecol Environ. 2019;17:400–406.
[48] Webb JS, Thompson LS, James S, et al. Cell death in Pseudomonas aeruginosa biofilm development. J Bacteriol. 2003;185:4585–4592.
[49] Tamaru Y, Takami Y, Yoshida T, et al. Crucial role of extracellular polysaccharides in desiccation and freezing tolerance in the terrestrial cyanobacterium Nostoc commune. Appl Environ Microbiol. 2005;71: 7327–7333.
[50] Wingender J, Jaeger K-E. Extracellular enzymes in biofilms. In: G Bitton, editor. Encyclopaedia of environmental microbiology. New York: Wiley; 2002. p. 1207–1223.
[51] Cadmus MC, Jackson LK, Burton KA, et al. Biodegradation of Xanthan gum by Bacillus Sp. Appl Environ Microbiol. 1982;44:5–11.
[52] Department of the Environment. Water, Heritage and the Arts, Commonwealth of Australia (DEWHA), Environmental risk assessment guidance manual for industrial chemicals; 2009.